Biochimica et Biophysica Acta 1837 (2014) 345–353

Contents lists available at ScienceDirect

Biochimica et Biophysica Acta

journal homepage: www.elsevier.com/locate/bbabio

Effect of constitutive expression of bacterial phytoene desaturase CRTI on photosynthetic electron transport in *Arabidopsis thaliana*

Denise Galzerano [a], Kathleen Feilke [a], Patrick Schaub [b], Peter Beyer [b], Anja Krieger-Liszkay [a,*]

[a] Commissariat à l'Energie Atomique (CEA) Saclay, iBiTec-S, CNRS UMR 8221, Service de Bioénergétique, Biologie Structurale et Mécanisme, 91191 Gif-sur-Yvette Cedex, France
[b] Faculty of Biology, University of Freiburg, 79104 Freiburg, Germany

ARTICLE INFO

Article history:
Received 28 May 2013
Received in revised form 28 November 2013
Accepted 19 December 2013
Available online 27 December 2013

Keywords:
bacterial phytoene desaturase
plastid terminal oxidase
photosynthetic electron transport
photoinhibition
reactive oxygen species
A. thaliana

ABSTRACT

The constitutive expression of the bacterial carotene desaturase (CRTI) in *Arabidopsis thaliana* leads to increased susceptibility of leaves to light-induced damage. Changes in the photosynthetic electron transport chain rather than alterations of the carotenoid composition in the antenna were responsible for the increased photoinhibition. A much higher level of superoxide/hydrogen peroxide was generated in the light in thylakoid membranes from the CRTI expressing lines than in wild-type while the level of singlet oxygen generation remained unchanged. The increase in reactive oxygen species was related to the activity of plastid terminal oxidase (PTOX) since their generation was inhibited by the PTOX-inhibitor octyl gallate, and since the protein level of PTOX was increased in the CRTI-expressing lines. Furthermore, cyclic electron flow was suppressed in these lines. We propose that PTOX competes efficiently with cyclic electron flow for plastoquinol in the CRTI-expressing lines and that it plays a crucial role in the control of the reduction state of the plastoquinone pool.

1. Introduction

When plants are exposed to light intensities exceeding the intensity needed to saturate photosynthetic electron transport, light-induced damage of the photosystems occurs [1,2]. The reaction center of photosystem II (PSII) is particularly susceptible to photoinhibition. Light-induced damage is caused by excessive production of reactive oxygen species such as singlet oxygen, superoxide, hydrogen peroxide and hydroxyl radicals [3,4]. Plants have developed several protective mechanisms to avoid photoinhibitory damage. These include short-term processes that modulate the structure and function of antenna complexes, comprising non-photochemical quenching (NPQ) of chlorophyll fluorescence, alternative electron transport pathways and movement of chloroplasts or even leaves away from intense light [5,6]. There are three components of NPQ: the qE type which depends on the reversible conversion of violaxanthin to zeaxanthin in the so-called xanthophyll cycle and on the protonation of the protein PsbS; state transitions (qT) and photoinhibition (qI) [7]. Changes in the xanthophyll content affect qE quenching as has been shown for a number of Arabidopsis mutants [8,9]. For instance, Arabidopsis mutants that lack lutein (*lut2*) exhibit a partial defect in qE while mutants with elevated lutein content show a larger qE [8,9]. Lutein has also been shown to be involved in the dissipation of excess light energy as heat in the light harvesting complex of photosystem II, LHCII [10].

Mutations and the constitutive overexpression of genes coding for carotenoid biosynthetic enzymes can affect the carotenoid composition in leaves. In lutein-deficient mutants *lut1* and *lut2* and in the neoxanthin and violaxanthin-deficient mutant *aba1*, the total carotenoid content remained unchanged and the xanthophylls reduced in amount were replaced by others [8]. Moreover, the *lut2* mutant exhibited alterations in PSII antenna size and had a reduced stability of the LHCII [11]. Constitutively expressing the bacterial phytoene desaturase CRTI in addition to the endogenous carotene desaturation pathway in rice and Arabidopsis resulted in a decrease in lutein, while the β-carotene-derived xanthophylls increased [12]. The mRNA levels of intrinsic carotenogenic enzymes remained unaffected in these plants [12]. In potato plants, the constitutive overexpression of CRTI and/or of the bacterial lycopene cyclase CRTY interfered negatively with leaf carotenogenesis also showing signs of chlorosis [13].

There is a functional connection between carotenoid biosynthesis and the reduction state of the photosynthetic electron transport chain since quinones are involved in plant-type phytoene desaturation [14,15]. In chloroplasts, the redox state of the plastoquinone pool is modulated by linear electron transport, by cyclic electron transport and by chlororespiration. It has been demonstrated that carotenoid biosynthesis

Abbreviations: 4-POBN, 4-pyridyl-1-oxide-N-tert-butylnitrone; Chl, chlorophyll; CRTI, phytoene desaturase; DCMU, 3-(3,4-Dichlorophenyl)-1,1-dimethylurea; DNP-INT, 2′-iodo-6-isopropyl-3-methyl-2′,4-4′-trinitrodiphenylether; Fm, maximum chlorophyll fluorescence signal; Fv, variable chlorophyll fluorescence signal; LHCII, light harvesting complex II; NDH, plastid NAD(P)H dehydrogenase; OG, octyl-gallate; P700, primary electron donor in PSI; PQ, plastoquinone; PS, photosystem; PTOX, plastid terminal oxidase; ROS, reactive oxygen species; TEMPD, 2,2,6,6-tetramethyl-4-piperidone hydrochloride

* Corresponding author at: CEA Saclay, iBiTec-S, Bât. 532, 91191 Gif-sur-Yvette Cedex, France. Tel.: +33 16908 1803; fax: +33 16908 8717.
E-mail address: anja.krieger-liszkay@cea.fr (A. Krieger-Liszkay).

0005-2728/$ – see front matter © 2013 Elsevier B.V. All rights reserved.
http://dx.doi.org/10.1016/j.bbabio.2013.12.010

is affected in mutants of the plastid terminal oxidase (PTOX) which oxidizes plastoquinol and transfers electrons to oxygen [16–18]. Furthermore, a tomato mutant deficient in the plastid NAD(P)H dehydrogenase (NDH) complex catalyzing non-photochemical electron fluxes to plastoquinone accumulated less carotenoids and had yellow-orange fruits [19]. In contrast, the bacterial CRTI which is inhomologous to plant-type desaturases, is an oxidase not involving quinones in the reaction mechanism [20].

Crti-overexpressing Arabidopsis lines differing in expression levels were obtained in previous work [12]. Among these, the plants with the highest level of CRTI showed an approximately 50% decrease in lutein content compared to the wt [12], partially compensated by β-carotene derived xanthophylls. We used these plants to investigate whether firstly, the alteration of the carotenoid composition increased their susceptibility to light and secondly, whether the redox state of the electron transport chain was altered. Since the plant-type carotene desaturation pathway is present in these plants in parallel to CRTI and the former, but not the latter, is dependent on PTOX at varying degrees, it is conceivable that the insertion of CRTI can indirectly through CRTI/PDS competition affect the reduction state of the plastoquinone pool. In this scenario, plastoquinones have dual functions in that they are integral constituents of photosynthetic electron transport besides being electron acceptors of the endogenous PDS (but not of the overexpressed CRTI).

To investigate the effect of CRTI insertion on the susceptibility of the plants to photodamage and on the reduction state of the plastoquinone pool, we followed non-photochemical quenching of chlorophyll fluorescence and photoinhibition of PSII by measuring the loss of variable fluorescence in leaves of wt and CRTI expressing lines in the presence or absence of the protein synthesis inhibitor lincomycin. Furthermore, we measured the post-illumination rise in chlorophyll fluorescence, thermoluminescence, P700 oxidation, and the light-induced generation of $^1O_2$ and of H_2O_2-derived hydroxyl radicals by spin trapping EPR spectroscopy. We demonstrate that the expression of CRTI increases the level of PTOX, promotes the generation of reactive oxygen species in chloroplasts and inhibits cyclic electron flow.

2. Materials and methods

2.1. Material

Arabidopsis thaliana (ecotype Columbia) plants were grown for 6–8 weeks in soil under short day conditions (8 h white light, 120 μmol quanta m^{-2} s^{-1}, 21 °C/16 h dark, 18 °C). We used two transgenic Arabidopsis lines expressing *crtI* under 35S promoter control as described in Schaub et al. [12]: the high expressing lines 2 (11) and 4 (14) were used in the present study. Line 14 has a higher *CrtI* expression level than line 11 (line 4 and line 2, respectively in [12]). For measurements on single leaves, we used plants from the same age and selected for the measurements leaves from the same age.

2.2. Extraction of thylakoid membranes and proteins from A. thaliana

2.2.1. Thylakoid membrane preparation

For thylakoid preparations, we used complete rosettes from 5 plants for each preparation. Leaves were ground in 0.33 M sorbitol, 60 mM KCl, 10 mM EDTA, 1 mM $MgCl_2$, 25 mM Mes pH 6.1. After centrifugation, the pellet was first washed with 0.33 M sorbitol, 60 mM KCl, 10 mM EDTA, 1 mM $MgCl_2$, 25 mM HEPES pH 6.7, then resuspended in 5 mM $MgCl_2$, 20 mM KPO_4 pH 7.6 to break intact chloroplasts. After centrifugation, the pellet was resuspended in 0.3 M sucrose, 5 mM $MgCl_2$, 20 mM KPO_4 pH 7.6 (measurement buffer) to a final concentration of 1 mg Chl ml^{-1}. All centrifugations were performed at 3,000 g for 3 min at 4 °C.

2.2.2. Protein extraction

Leaves were ground in liquid nitrogen before homogenization in lysis buffer. The lysis buffer contained 100 mM Tris–HCl pH 6.8, 4% SDS, 20 mM EDTA, protease inhibitor cocktail (Sigma-Aldrich, St-Louis, Missouri, United States). Samples were then centrifuged for 15 min, 10,000 g at 4 °C to remove the cell debris and the supernatants were recovered.

2.3. Pigment analysis

For each analysis, 10 leaves of the same age from 5 different plants were collected, lyophilized and ground to a fine powder using a stone mill (MM200, Retsch, Germany) at 30 Hz for 1 min. 5–10 mg of leaf sample were extracted with 2 ml Tris-buffered acetone (10 vol% 100 mM Tris) by sonication. After centrifugation for 5 min at 3000 g the supernatant was transferred to a new tube and the remaining pellet re-extracted twice with 2 ml acetone, each. The combined extracts were mixed with 2 ml PE:DE (2:1, v,v) and partitioned twice against a 1% (w/v) sodium chloride solution. The combined organic phases were dried and dissolved in 100 μl chloroform out of which five μl were subjected to quantitative analysis using a Shimadzu Prominence UPLC system with a YMC C30 150 x 2.1 reversed-phase column (YMC Europe GmbH, Germany). The gradient system employed A: MeOH/tert-butylmethylether (TBME)/water 30:1:10 (v/v/v) and B: MeOH/TBME 1:1 (v/v). The gradient started at 100% A, followed by a linear gradient to 0% A within 20 min at a flow-rate of 0.5 ml min^{-1}. An isocratic segment run for 4 min at 0% A, completed the run. For quantitative analyses, 5 μg VIS682A (QCR Solutions, USA) were added to each sample as an internal standard prior to extraction. All peaks were normalized relative to the internal *VIS682A* standard to correct for extraction and injection variability. A β-carotene calibration curve, run separately, was used to calculate carotenoid amounts. All carotenoid peaks were integrated at their individual λ_{max} and underwent a second normalization to correct for their individual molar extinction coefficients relative to β-carotene (=1), using violaxanthin (1.01), lutein-epoxyd (0.96), antheraxanthin (1.01), lutein (1.09), chlorophyll *a* (1.48) and chlorophyll *b* (1.00). Carotenoids were identified by their retention times and absorption spectra, monitored using a photodiode array detector (Shimadzu Prominence UPLC system, München, Germany).

2.4. O_2 measurements

Measurements of O_2 production and consumption were performed in a Liquid-Phase Oxygen Electrode Chamber (Hansatech Instruments, Norfolk, England). Total electron transport activity was measured as O_2 evolution using thylakoids (10 μg Chl/ml) in the presence of 1 mM $K_3[Fe(CN)_6]$, PSII activity was measured in the presence of 1 mM 2,6-dichloro-1,4-benzoquinone and 0.5 mM $K_3[Fe(CN)_6]$. PSI activity was measured in the presence of 10 μM DCMU, 5 mM ascorbate, 30 μM 2,6-dichlorophenol-indophenol and 500 μM methylviologen. All activities were measured in the presence of 5 μM nigericin as uncoupler.

2.5. Chlorophyll fluorescence

Room temperature chlorophyll fluorescence was measured using a pulse-amplitude modulation fluorometer (DUAL-PAM, Walz, Effeltrich, Germany). As actinic light, red light at 635 nm was used. The intensity of the measuring light was sufficiently low (integral intensity about 9 μmol quanta m^{-2} s^{-1}, frequency of modulated light) to prevent the stable reduction of plastoquinone. Saturating flashes (1 s) were given to probe the maximum fluorescence level. The maximum quantum yield of PSII, Fv/Fm, was assayed by calculating the ratio of the variable fluorescence, Fv, to the maximal fluorescence, Fm, in the dark-adapted state. Photochemical (qP) and non-photochemical quenching (NPQ) was assayed during 5 min of actinic light (660 μmol quanta m^{-2} s^{-1}), followed by a recovery period of 3 min. NPQ was

defined as (Fm–Fm′)/(Fm–Fo′) with Fm′ being the maximal fluorescence in the actinic light and qP as (Fm′–F)/(Fm–Fo′). Plants were taken from the growth chamber during the light period and dark-adapted for 10 min prior to the measurement to allow most of the reversible quenching to relax.

The F_0' rise in the dark was measured after illumination with actinic red light (I = 825 μmol quanta m^{-2} s^{-1}). After 10 min actinic light, the measuring light was set on and the actinic light was switched off.

2.6. Photoinhibition

Photoinhibition of PSII was carried out on detached leaves at 1000 μmol quanta m^{-2} s^{-1}. To block chloroplast-encoded protein synthesis, detached leaves were vacuum-infiltrated with lincomycin (1 g l^{-1}) and floating on the lincocmycin solution for 3 h in dim light prior to the photoinhibitory treatment. During the photoinhibition treatment leaves were kept hydrated on wet filter paper. As a measure of PSII activity Fv/Fm was determined.

2.7. Thermoluminescence

Thermoluminescence was measured with a home-built apparatus on leaf segments taken from plants and dark-adapted for 5 min. Thermoluminescence was excited with single turnover flashes at 1 °C spaced with a 1 s dark interval. Samples were heated at a rate of 20 °C/min to 70 °C, and the light emission was recorded. Graphical and numerical data analyses were performed according to Ducruet and Miranda [21].

2.8. P_{700} measurements

The redox state of P_{700} was monitored by following changes in absorbance at 830 nm using a DUAL-PAM. Leaves attached to the plants were used. The plants were kept in the light in the growth chamber so that the Calvin–Benson cycle enzymes were activated and were dark-adapted for 15 min prior to the measurements. To probe the maximum extent of P_{700} oxidation leaves were illuminated with far-red light (190 μmol quanta m^{-2} s^{-1}, highest light intensity provided by the DUAL-PAM). At each intensity of actinic light, the increase in absorption was followed until a constant level was reached.

Kinetics of P700 oxidation were probed by far-red illumination. For this assay, plants were dark-adapted for 10 min, then preilluminated for 3 min with red light (I = 600 μmol quanta m^{-2} s^{-1}). After this pre-illumination the P_{700} measurement was started using the following illumination protocol: 10 s dark, 5 s actinic red light (I = 600 μmol quanta m^{-2} s^{-1}), 2 s dark, 17 s far-red light (highest intensity of the DUAL-PAM). Only the first seconds after onset of far-red light are shown in Fig. 11. The amplitudes of the signals were normalized to the signal size of wt.

2.9. Room-Temperature EPR Measurements

Spin-trapping assays with 4-pyridyl-1-oxide-*N*-*tert*-butylnitrone (4-POBN) (Sigma-Aldrich) to detect the formation of hydroxyl radicals were carried out using thylakoid membranes at a concentration of 10 μg Chl ml^{-1}. Samples were illuminated for 2 min with red light (RG 630) (500 μmol quanta m^{-2} s^{-1}) in the presence of 50 mM 4-POBN, 4% ethanol, 50 μM Fe-EDTA, and buffer (20 mM phosphate buffer, pH 7.5, 5 mM $MgCl_2$, 0.3 M sorbitol). When required, 10 μM octyl gallate was added prior to the illumination.

To detect singlet oxygen, samples (10 μg Chl ml^{-1}) were illuminated for 2 min with red light (RG 630) (1000 μmol quanta m^{-2} s^{-1}) in the presence of 100 mM of the spin probe 2,2,6,6-tetramethyl-4-piperidone hydrochloride (TEMPD).

EPR spectra were recorded at room temperature in a standard quartz flat cell using an ESP-300 X-band spectrometer (Bruker, Rheinstetten, Germany). The following parameters were used: microwave frequency 9.73 GHz, modulation frequency 100 kHz, modulation amplitude: 1 G, microwave power: 63 milliwatt in TEMPD assays, or 6.3 milliwatt in 4-POBN assays, receiver gain: $2x10^4$, time constant: 40.96 ms; number of scans: 4.

2.10. Immunoblots

Leaf extracts were used for analysis by SDS-PAGE (12% acrylamide) and immunoblotting. Proteins were blotted onto nitrocellulose filters. Labeling of the membranes with anti-PTOX (generous gift from Marcel Kuntz, Grenoble), anti-ATP-B (Agrisera, Vännäs, Sweden) or anti-NDH-H (generous gift from Dominique Rumeau, CEA Cadarache) was carried out at room temperature in 1x TBS (50 mM Tris–HCl pH 7.6, 150 mM NaCl), 0.1% Tween 20 and 5% non-fat milk powder. After washing, bound antibodies were revealed with a peroxidase-linked secondary anti-rabbit antibody (Agrisera, Vännäs, Sweden) and visualized by enhanced chemiluminescence. The density of the bands was analyzed using the program ImageJ.

3. Results

3.1. Light sensitivity of CRTI expressing lines

We investigated the light sensitivity of Arabidopsis lines which expressed the bacterial phytoene desaturase (CRTI) constitutively in addition to their endogenous plant desaturases. We used two high CRTI expressing lines (named herafter CTRI-lines, see Materials) which showed the strongest relative reduction in their lutein proportion [12]. These lines showed growth retardation (Fig. 1; fresh weight wt: 100 ± 23%; line 11: 77 ± 21%; line 14: 48 ± 9%; n = 22) when grown under short day conditions (8 h light/16 h dark), and the leaves were paler. Pigment analysis (Fig. 2) showed that the total carotenoid content in leaves from the CRTI-lines decreased from 2.38 μg/mg dry mass to 2.05 μg/mg dry mass in the CRTI-lines. The CRTI-lines contained about 50% less lutein as has been published previously [12]. A part of the missing lutein was replaced by violaxanthin and antheraxanthin. The β-carotene content remained unchanged. In addition to these changes in the carotenoid composition, the chlorophyll content was slightly decreased. Chl b decreased by 9–10% in both CRTI-lines, Chl a by 10–14%

Fig. 1. Phenotypes of *Arabidopsis thaliana* wild-type (wt), CRTI-lines 11 and 14 after 7 weeks grown on soil.

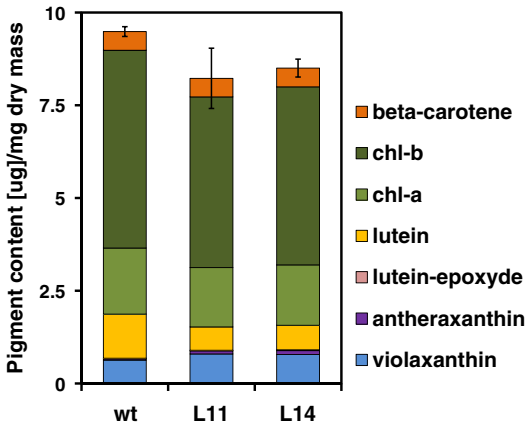

Fig. 2. Chlorophyll and carotenoid content of mature leaves from wt and CRTI-lines 11 and 14. Each bar represents a pool of extracts made from mature leaves from five different plants. The mean of three measurements are shown (n = 3 ± SE).

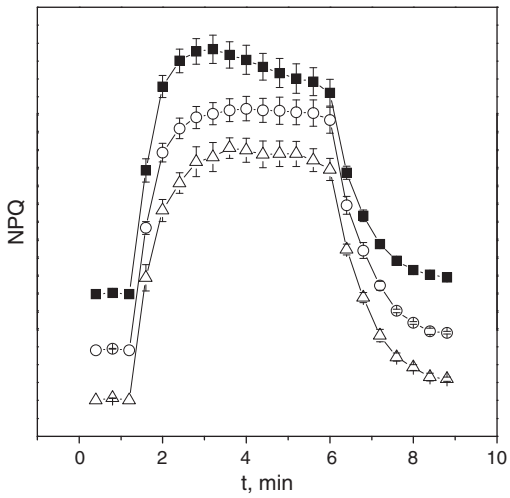

Fig. 3. Non-photochemical (NPQ) quenching in wt (filled squares), CRTI-lines 11 (circles) and 14 (triangles). Dark-adapted leaves were illuminated with red light (I = 660 μmol quanta m^{-2} s^{-1}) and chlorophyll fluorescence was measured on leaves still attached to the plant. Curves of each line were displaced vertically. Individual plants were measured (n = 3 ± SE).

in line 11 and 14, respectively. Changes in the carotenoid composition did not lead to changes in activity of the main complexes of the photosynthetic electron transport chain measured in the presence of an uncoupler. In isolated thylakoid membranes from wt and the two CRTI-lines the total electron transport activity was 97 ± 7 μmol O_2 mg chl^{-1} h^{-1}, the PS II activity was 108 ± 5 μmol O_2 mg chl^{-1} h^{-1} and the PSI activity was 345 ± 7 μmol O_2 mg chl^{-1} h^{-1}. These values show that the ratio of PSII:PSI was unaltered in the CRTI-lines.

However, measurements of chlorophyll fluorescence showed that the quantum efficiency of PSII was slightly lowered in the two CRTI-lines (Table 1). This may be taken as an indication for a more light-sensitive PSII. When leaves were exposed to high light (1000 μmol quanta m^{-2} s^{-1}) for 1 h in the presence of lincomycin to inhibit synthesis of the D1 protein, leaves from the CRTI-lines showed a higher loss of Fv/Fm than wt (Table 1). A higher susceptibility to light may be caused by alteration in the antenna, of NPQ and of the yield of $^1O_2$ generation or by alterations in the photosynthetic electron transport chain. To investigate whether the lower lutein content of the antenna influences the ability of the plants to dissipate excess energy by non-photochemical quenching, chlorophyll fluorescence curves were analyzed in more detail. As shown in Fig. 3, the CRTI-lines showed a slower induction of NPQ than wt while the total extent of NPQ and also the photochemical quenching (qP) (not shown) were not affected. A change in NPQ is supposed to lead to a higher yield of $^1O_2$ generation as has been shown for the npq4 mutant [22]. The generation of $^1O_2$ during 2 min of illumination was followed by spin trapping EPR spectroscopy in thylakoid membranes from the the CRTI-lines and wt. Fig. 4 shows typical EPR spectra of the spin adduct TEMPDO which results from the reaction of 2,2,6,6-tetramethyl-4-piperidone hydrochloride (TEMPD) with $^1O_2$ [23]. Illumination of thylakoid membranes of wt and the two CRTI-lines gave approximately the same signal size. This shows that although the carotenoid composition of the thylakoid membranes was altered [12], the yield of light-induced $^1O_2$ generation remained unchanged.

Table 1
Photoinhibition of PSII in leaves from wild-type and the CRTI-lines 11 and 14.
Leaves were subjected to high light illumination (I = 1000 μmol quanta m^{-2} s^{-1}) for 1 h. The maximum quantum yield of PSII (Fv/Fm) was determined before and after the high light exposure. Prior to the measurements, leaves had been infiltrated with lincomycin and were dark-adapted for 10 min before measuring fluorescence. Error bars represent SE (7 independent experiments). After 1 h high light treatment, Fv/Fm values of the CRTTI-lines are significantly different to wt ($P < 0.01$).

sample	Fv/Fm before high light	Fv/Fm after high light
wt	0.83 ± 0.01	0.66 ± 0.02
Line 11	0.78 ± 0.03	0.57 ± 0.02
Line 14	0.77 ± 0.04	0.51 ± 0.03

Thus, the higher susceptibility to photoinhibition cannot be explained by a higher yield of $^1O_2$ formation. Moreover no substantial alterations in the antenna composition (LHCII monomers and trimers) were observed when PSII-enriched membrane fractions of wt and the CRTI-lines were compared (SI Fig. 1). It has to be noted that although at 77 K the ratio between the fluorescence emission at 730 nm (reflecting PSI) and the fluorescence emission at 685 nm and 695 nm (reflecting PSII) was unchanged between wt and the CRTI-lines, there was a change in the relative intensity of the fluorescence emitted at 685 nm and that at 695 nm in the CRTI-lines. This may indicate that the coupling of the LHCII is slightly perturbed in the CRTI-lines leading to stronger emission of fluorescence from CP47 at 695 nm [24] for unknown reasons.

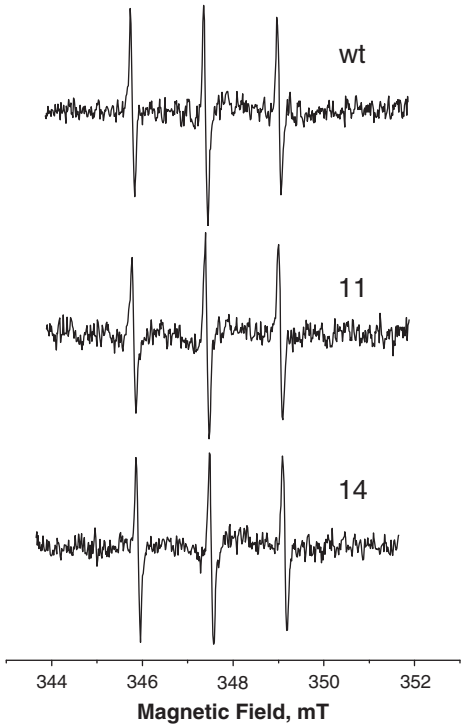

Fig. 4. Generation of $^1O_2$ in isolated thylakoids from wild-type and CRTI-lines 11 and 14. Samples were illuminated in the presence of 100 mM TEMPD for 2 min with 1000 μmol quanta m^{-2} s^{-1} red light, filtered by RG 630. Typical EPR spectra are shown.

3.2. Generation of H_2O_2-derived hydroxyl radicals in the CRTI-lines

Next we investigated whether other ROS may be responsible for the observed phenotype in the insertion lines. Superoxide ($O_2^{\bullet-}$), hydrogen peroxide (H_2O_2) and hydroxyl radicals ($HO^{\bullet}$) can be generated by the reduction of O_2 in photosynthetic electron transfer in a number of different reactions: O_2 can act as terminal acceptor in the so-called Mehler reaction at the acceptor side of PSI [25], it can be reduced by plastosemiquinones in the membrane [26], it can be reduced at the acceptor side of PSII [27] and it is the electron acceptor of the plastid terminal oxidase (PTOX) which uses plastoquinol as electron donor. During photosynthetic electron transport the reduction of O_2 to $O_2^{\bullet-}$ may occur under conditions of limited electron acceptor availability other than O_2. Two molecules of $O_2^{\bullet-}$ dismutate, either spontaneously or catalyzed by superoxide dismutase, to H_2O_2 and O_2. In the presence of reduced transition metal ions such as Fe^{2+}, H_2O_2 gives rise to the hydroxyl radical ($HO^{\bullet}$) supported by the reduction of Fe^{3+} by $O_2^{\bullet-}$ (Haber–Weiss reaction). We investigated the light-induced formation of $O_2^{\bullet-}/H_2O_2$ by EPR spectroscopy using ethanol/4-POBN as spin trap. FeEDTA was added as catalyst of the Haber–Weiss reaction. Performing 4-POBN spin trapping in the presence of ethanol is a general procedure to indirectly prove the formation of $HO^{\bullet}$ through the detection of the secondary 4-POBN/α-hydroxyethyl spin adduct. Whereas little or no signal was observed when samples were maintained in the dark in the presence of ethanol/4-POBN, illumination of thylakoids resulted in strong EPR signals giving sextets of lines ($a_N = 15.61$ G; $a_{H\beta} = 2.55$ G) characteristic of the 4-POBN/α-hydroxyethyl aminoxyl radical (Fig. 5). In the absence of FeEDTA, no EPR signal was detected, showing that the detected radical originates from $O_2^{\bullet-}/H_2O_2$. CRTI-lines produced a signal which was approximately 50% larger than the signal obtained from wt thylakoids after 5 min illumination with 500 μmol quanta m^{-2} s^{-1} white light (Table 2). Addition of DCMU, an inhibitor that binds to the Q_B-binding pocket in PSII thereby blocking linear electron transport, almost completely inhibited spin adduct formation. This shows that ROS were generated by photosynthetic electron transfer reactions beyond PSII. In the presence of DNP-INT, an inhibitor of the cytochrome b_6f complex, about 80% of the EPR signal was lost in the wt and about 60% in the CRTI-lines, showing that the main site of ROS generation is localized at the acceptor side of PSI. However, still a significant amount of ROS was detected when the electron transport was blocked at the level of the cytochrome b_6f complex. This site of ROS production was more important in the CRTI-lines than in the wt. Superoxide may be generated by reduced plastoquinone, especially when it is in its semi-reduced form ($PQH^{\bullet-}$) or by the action of PTOX. It has been shown that the overexpression of PTOX in tobacco leads to $O_2^{\bullet-}$ generation [28]. In addition, it has been reported recently that a tobacco line that expresses PTOX from *Chlamydomonas reinhardtii* suffers from photoinhibition [29]. To test whether ROS generation is stimulated in the CRTI-lines, octyl gallate, a specific inhibitor of PTOX, was added to the samples. As shown in Fig. 6, the formation of the EPR signal was largely suppressed by octyl gallate. The effect of octyl gallate was larger in the transgenic lines than in the wt (Table 2). Immunoblots show that the PTOX content was increased in the insertion lines compared to wt while the amount of the NDH complex showed no significant change (Fig. 7).

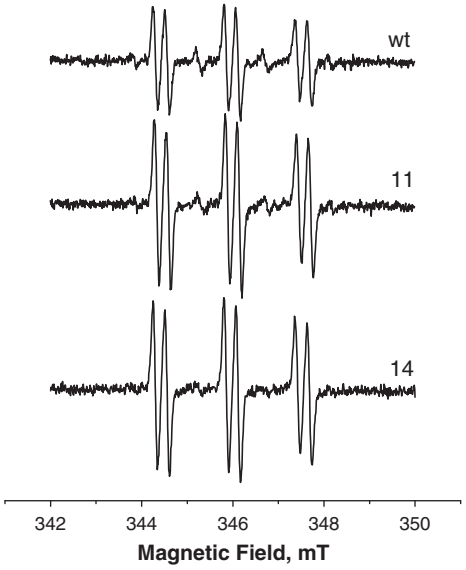

Fig. 5. Light-induced hydroxyl radical formation in thylakoids from wt and the CRTI-lines 11 and 14. Generation of hydrogen peroxide-derived hydroxyl radicals was measured by indirect spin trapping with 4-POBN/ethanol. Representative EPR spectra of the 4-POBN/α-hydroxyethyl adduct are shown. Samples were illuminated for 5 min with white light (500 μmol quanta m^{-2} s^{-1}).

Table 2
Hydroxyl radical production in isolated thylakoids from wild-type, line 11 and line 14. Thylakoids were illuminated for 5 min with white light (500 μmol quanta m^{-2} s^{-1}) in the presence of the spin trap 4-POBN, ethanol and FeEDTA. When indicated, 10 μM DCMU, 100 μM DNP-INT and/or 10 μM octyl gallate (OG) were added prior to the illumination. In the absence of inhibitors, the double integral of the total signal obtained with each type of sample was normalized to the wt. The signal sizes in the presence of the inhibitors were normalized to the corresponding signal sizes in the absence of the inhibitors. SE is given, n = 8 independent experiments of different thylakoid preparations from three different growth sets.

sample	EPR signal size (norm.)
wt	1
11	1.48 ± 0.08
14	1.50 ± 0.05
wt + DCMU	<0.03
11 + DCMU	<0.03
14 + DCMU	<0.03
wt + DNP-INT	0.20 ± 0.06
11 + DNP-INT	0.37 ± 0.04
14 + DNP-INT	0.42 ± 0.05
wt + OG	0.73 ± 0.07
11 + OG	0.61 ± 0.05
14 + OG	0.59 ± 0.05
wt + DNP-INT + OG	0.07 ± 0.02
11 + DNP-INT + OG	0.06 ± 0.02
14 + DNP-INT + OG	0.05 ± 0.02

3.3. Reduction state of the plastoquinone pool in CRTI-lines

An increase in PTOX abundance can be interpreted as a response of the system to maintain the PQ pool in a more oxidized state. One possibility to measure the reduction state of the PQ pool is to follow the transient increase of the chlorophyll fluorescence level after a short period of illumination of the leaves with actinic light. In the light, $NADP^+$ is reduced and immediately after offset of the light, electrons are fed via the NDH complex into the PQ pool [30]. The chlorophyll fluorescence level increases because the plastoquinol is in equilibrium with the plastoquinone molecules at the acceptor side of PSII. An increase of F_0' indicates the reduction of the primary quinone acceptor Q_A by the highly reduced plastoquinone pool. The rise of F_0' after illumination with actinic light was followed to test for an enhanced PTOX activity in the CRTI-lines. Fig. 8 shows that, in the absence of the PTOX inhibitor octyl gallate, the F_0' rise was clearly visible in the wt, while it was much lower in the CRTI-line 14 and completely suppressed in line 11. The F_0' rise was restored in both CRTI-lines by the addition of octyl gallate. This shows that, after exposure to actinic light, the PQ pool is more oxidized in the dark in the CRTI-lines compared to wt. Infiltration of the leaves with octyl gallate had no effect on the Fv/Fm values (data not shown). The F_0' rise after illumination shows qualitatively the re-reduction of the PQ pool via the NDH complex or via a different metabolic route. We performed as a second test thermoluminescence measurements to probe the reduction of the plastoquinone pool in the dark and to demonstrate further that the PTOX activity was higher in the two

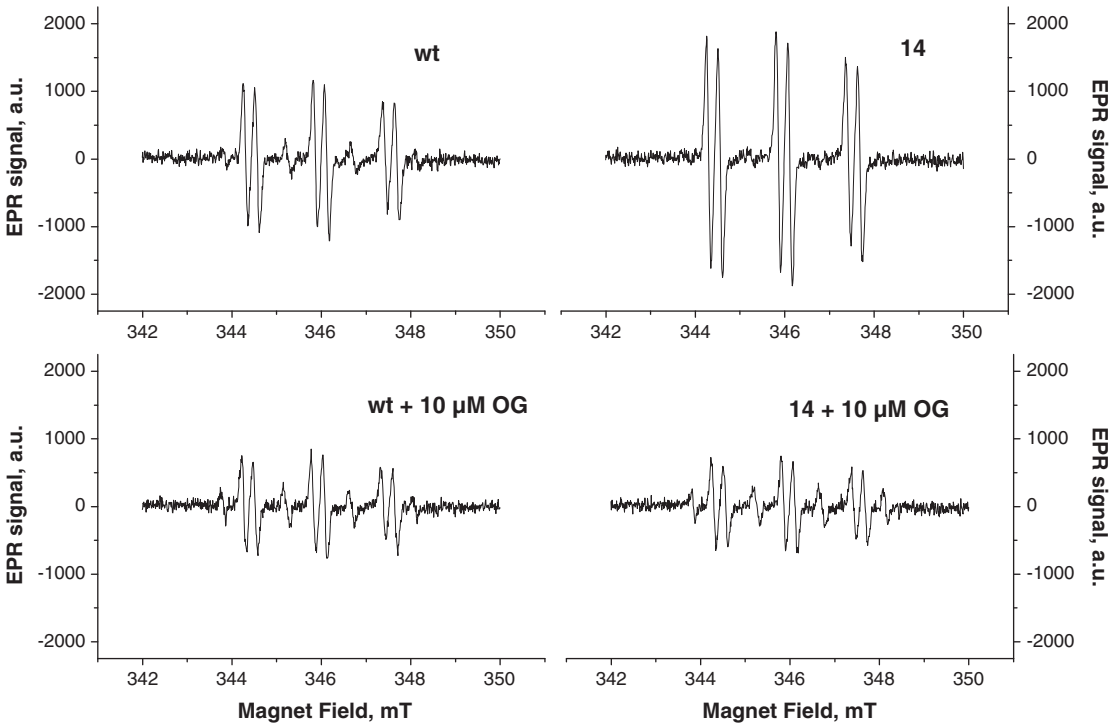

Fig. 6. Light-induced hydroxyl radical formation in thylakoids from wt and line 14 in the presence and absence of 10 μM octyl gallate (OG). Generation of hydrogen peroxide-derived hydroxyl radicals was measured by indirect spin trapping with 4-POBN/ethanol. Typical EPR spectra of the 4-POBN/α-hydroxyethyl adduct are shown. Samples were illuminated for 5 min with white light (500 μmol quanta m^{-2} s^{-1}).

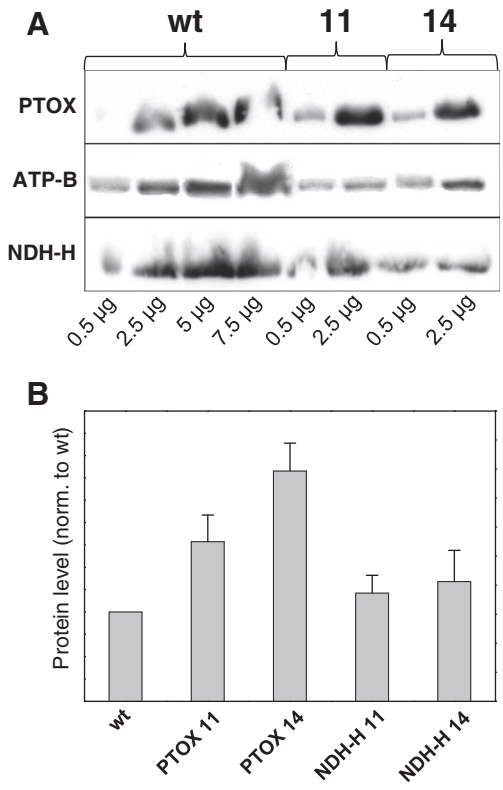

Fig. 7. PTOX content in wt and the CRTI-lines 11 and 14. Protein composition of the protein extracts from leaves was analyzed by SDS-PAGE and immunoblotting with antisera against PTOX, the β-subunit of ATP-synthase and NDH-H. Leaf extracts were used. A: a typical immunoblot; B: Density of the bands recognized by anti-PTOX and anti-NDH-H in lines 11 and 14 were normalized to the density measured in wt (mean ± SE). In case of PTOX 6 immunoblots and in case of NDH-H 4 immunoblots, each with proteins from different preparations, were used for the statistical analysis. Gels were loaded based on chlorophyll content.

CRTI-lines than in the wt. As shown in Fig. 9, leaves of the CRTI-lines showed a very different profile of the luminescence emission after three single turnover flashes than the wild-type. The thermoluminescence curve of wt could be fitted by two bands, the first with a temperature maximum between 25–30 °C, characteristic of the B-band ($S_{2/3}Q_B^-$ recombination, with $S_{2/3}$ being oxidation states of the Mn cluster and Q_B being the secondary quinone electron acceptor of PSII) [31], and the second band with a temperature maximum at about 45 °C, the so-called afterglow band (AG-band) [32]. The AG-band is detected in samples in which cyclic electron flow is active [33], so that the PQ pool becomes reduced in the dark. The intensity of the AG-band relative to the B-band is highest after the third excitation flash [34]. While the AG-band was clearly visible in the wt, it was suppressed in the two CRTI-lines (Fig. 9) indicating that the increased level and activity of PTOX do not allow the accumulation of PQH_2 in the dark.

3.4. Cyclic electron flow in the CRTI-lines

Since the lack of the AG-band in the CRTI-lines indicates a low re-reduction of the PQ pool in the dark and since this is interpreted to reflect the activity of the cyclic electron flow in the light [33], we tested the activity of cyclic electron flow in the CRTI-lines compared to wt. Cyclic electron flow operates via two different routes, one involving a plastoquinone reductase which is homologous to the mitochondrial complex I, the so-called NDH complex, and the other via a putative ferredoxin-quinone reductase, feeding electrons directly into the cytochrome b_6f complex, the so-called PGRL1/PGR5-dependent pathway [35] (for a recent review see Johnson, [36]). Cyclic electron flow may be affected in the insertion lines because PTOX may compete with the cytochrome b_6f complex for the substrate PQH_2.

Figs. 10, 11 show absorption measurements of leaves at 830 nm which are indicative for the oxidation state of P_{700}. In Fig. 10, the maximum signal of P_{700}^+ was probed for each leaf with far-red light which preferentially excites PSI. The far red illumination was followed by illumination with increasing intensities of actinic red light and the

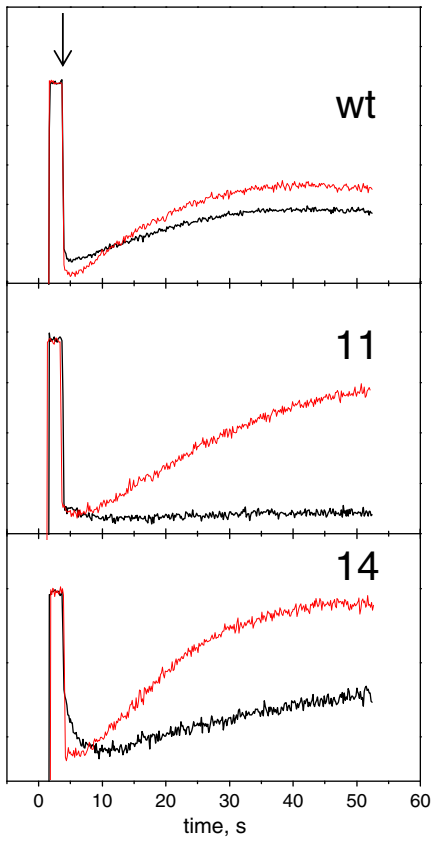

Fig. 8. F_0' rise after illumination with actinic light in leaves from wt and the CRTI-lines 11 and 14. Leaves were vacuum-infiltrated with water (black line) or with 50 μM octyl gallate (red line) and dark-adapted on damped tissue paper for 3 h. Then they were illuminated with red actinic light (I = 825 μmol quanta m^{-2} s^{-1}) for 10 min. After 10 min, the measuring light was set on, the actinic light was switched off (arrow) and the F_0' rise was followed. Typical traces, each from an individual leaf, are shown.

maximum level of P_{700}^+ formation was plotted for each light intensity. As shown in Fig. 10, the extent of P_{700} oxidation in the wild-type was slightly lower at a given light intensity than in the CRTI-lines 11 and 14. Even at the highest light intensity, the signal of P_{700}^+ was lower than the value obtained with far-red light. The difference between the wt and the CRTI-lines was small but significant. This indicates active cyclic electron flow to take place in wt leaves in contrast to leaves from the CRTI-lines. A lower extent of P_{700} formation at high light intensities may alternatively be explained by charge recombination events taking place in the reaction center of PSI from wt and not in those from the CRTI-lines. To support our hypothesis that the lower extent

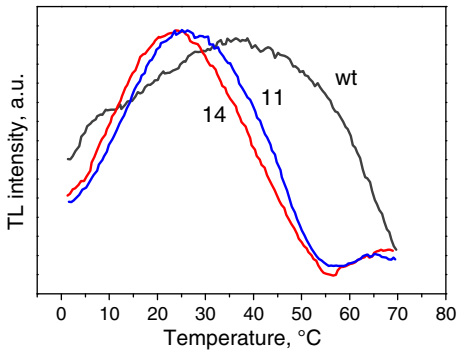

Fig. 9. Thermoluminescence measurements of dark-adapted leaves. Black line: wild-type; blue: CRTI line 11; red: CRTI line 14. Samples were excited by three single turnover flashes spaced with 1 s interval.

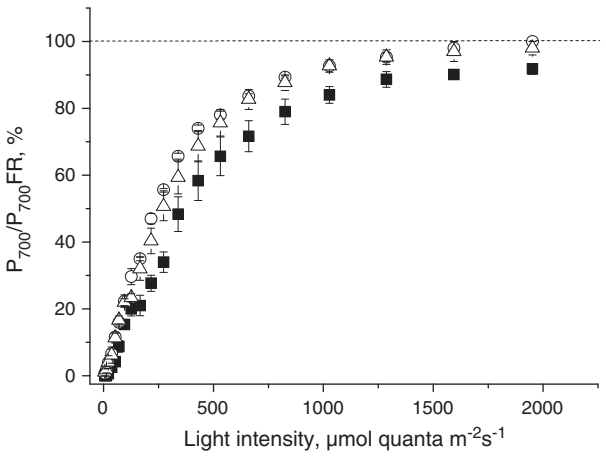

Fig. 10. Dependence of PSI oxidation on the intensity of actinic light. Leaves from wt (filled squares), CRTI line 11 (circles) and CRTI line 14 (triangles) were illuminated at 120 μmol quanta m^{-2} s^{-1} for at least 1 h and then dark-adapted for 15 min prior to the measurements. Leaves were first illuminated with far red light (FR) to obtain the maximum signal corresponding to P_{700}^+ formation (n = 4–6 ± SE).

of P_{700} oxidation was caused by cyclic electron flow, we followed the kinetics of P_{700} oxidation by far-red light in wt and the CRTI-lines (Fig. 11). This method shows the activity of cyclic flow onset of light and not during steady state conditions. In the CRTI-lines, the oxidation of P_{700} by far-red illumination was faster than in the wt, further demonstrating that fewer electrons were available for reducing P_{700}^+ and that thus cyclic flow was suppressed in these lines.

4. Discussion

Here we show that the constitutive expression of the bacterial carotene desaturase CRTI in addition to the endogenous desaturases leads to a higher susceptibility of PSII to photodamage (Table 1) and to an increased level and activity of PTOX (Figs. 6–9). The increase in PTOX activity causes a higher yield of $O_2^{\bullet-}/H_2O_2$ formation (Figs. 5, 6, Table 2). In contrast to these results, PTOX has been proposed previously to act as a safety valve keeping the PQ pool oxidized and avoiding thereby photooxidative damage [37]. Especially under harsh environmental conditions like in alpine plants [38,39], plants exposed to extreme temperatures [40,41] or to high salinity [42], the PTOX protein level is increased and PTOX seems to play an important role in allowing

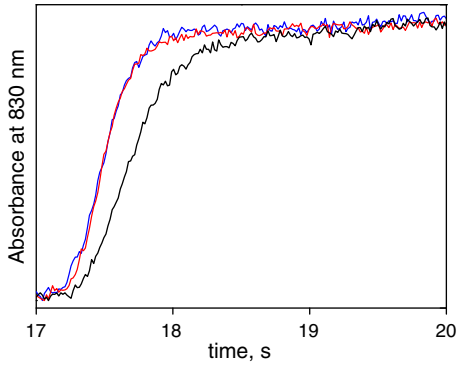

Fig. 11. PSI oxidation was probed by far-red illumination in wt and CRTI-lines 11 and 14. Plants were dark-adapted for 10 min, then preilluminated for 3 min with red light (I = 600 μmol quanta m^{-2} s^{-1}). After the preillumination the P_{700} measurement with the DUAL-PAM was started using the following illumination protocol: 10 s dark, 5 s actinic red light (I = 600 μmol quanta m^{-2} s^{-1}), 2 s dark, 17 s far-red light (highest intensity of the DUAL-PAM). Only the first seconds after onset of far-red light are shown. The amplitudes of the signals were normalized to the signal size of the wild-type. Black: wt, blue: line 11, red: line 14. Typical traces are shown.

the plant to adapt to the stress condition. However, in model plants like Arabidopsis and Tobacco grown under standard conditions, the role of PTOX is less clear. Overexpression of PTOX in Arabidopsis did not improve the susceptibility of the plants against photoinhibition [43] or even triggered photoinhibition in tobacco [28,29].

The question arises whether the increase in $O_2^{\bullet-}/H_2O_2$ generation as shown here and in tobacco overexpressing PTOX [28] or the suppression of cyclic electron flow (Figs. 10, 11) is responsible for increased photodamage. As shown in Table 2, most of $O_2^{\bullet-}/H_2O_2$ are generated at the acceptor side of PSI in the Mehler reaction since the cytochrome b_6f inhibitor DNP-INT inhibits approximately 60% of the ROS formation in the CRTI-lines. We attribute the proportion that is still detectable in the presence of DNP-INT to the action of PTOX since the PTOX inhibitor octyl gallate has a stronger effect on the CRTI-lines than on wt (Fig. 6, Table 2). At present, we cannot decide whether PTOX itself produces reactive oxygen species as a side product of the reduction of oxygen or whether reactive oxygen species are produced by the semiplastoquinone $PQH^{\bullet-}$ or, in vivo, by a higher activity of the Mehler reaction. The difference in the signal size between the signals obtained in the absence and in the presence of octyl gallate corresponds to about 3 μmol H_2O_2 mg Chl^{-1} h^{-1}. It is questionable whether this amount is sufficient for triggering photoinhibition of PSII. As shown in Figs. 10 and 11, less cyclic electron flow is detectable in the CRTI-lines. Cyclic electron flow protects against photodamage of PSI since it keeps its acceptor side oxidized [1,44–46]. Furthermore, it participates also in the photoprotection of PSII by 1) contributing to the generation of the proton gradient across the thylakoid membrane and thereby to NPQ and by 2) limiting the $O_2^{\bullet-}$ generation at the acceptor side of PSI. $O_2^{\bullet-}$ generated at PSI has been shown to damage PSII [4]. Since the amount of $^1O_2$ produced is not increased in the CRTI-lines, we suggest that the higher photodamage is caused by both, the suppression of the cyclic flow and the increased $O_2^{\bullet-}/H_2O_2$ level.

Arabidopsis mutants that lack PTOX show a variegated phenotype and were called *immutans* (*im*) with the white plastids accumulating phytoene in leaf sectors [16,17,47,48]. Mutants of cyclic electron flow defective in the activity of NDH complex or/and lacking PGR5, a thylakoid protein involved in cyclic electron transport, rescued *im* variegation [49]. This indicates that the redox state of the PQ pool has to be very well controlled to allow optimal photosynthetic electron transport activities in vivo. A too reduced PQ pool as in the case of *im* with functional cyclic flow renders leaves more susceptible to photoinhibition. It has been shown recently using the *ghost* mutant in tomato which lacks PTOX that PTOX modulates the balance between linear and cyclic flow rather than acting as a safety valve [50]. These authors suggest that the concerted action of the NDH complex and PTOX is important to set the redox poise in the thylakoid membrane. In the CRTI-lines, the amount of PTOX is increased while the amount of the NDH complex is unchanged. The PQ pool is held so oxidized that less electron donors for cyclic flow are available, a condition which facilitates photoinhibition. It is unknown whether PTOX oxidizes plastoquinol independent of the PQH_2 localization in the thylakoid membrane or whether it oxidizes PQH_2 in well-defined regions of the membrane. PTOX has been shown to be localized in the stroma lamellae [51]. and may therefore preferentially oxidize PQH_2 implicated in cyclic electron flow. In analogy to the supercomplex found in state 2 in Chlamydomonas [52], a tight coupling between cytochrome b6f complex and PSI may also be required in higher plants for cyclic electron flow to operate.

It remains to be clarified why the constitutive expression of CRTI exerts such profound effects on PTOX levels and activity and consequently on plastoquinone redox-homeostasis. It is conceivable that two pathways of carotene desaturation, the endogenous pathway via PDS and the added pathway via CRTI, are in competition. CRTI is, in fact, active in chloroplasts as has been shown several times including this work: norflurazon treatment blocking PDS allows carotenoids to form through CRTI. Pigment analysis showed that the pigment composition in the CRTI-line 14 was not altered by norflurazon (SI Fig. 3). Assuming that the PDS route is kept less "busy" by the additional catalysis of CRTI, all measured consequences need to be traced back to the mechanistic differences existing between the two.

CRTI is a bacterial phytoene desaturase that is distinct from the cyanobacterial/plant carotene desaturation system. With the exception of the FAD-binding domain, CRTI shares no sequence homology with plant desaturases. Mechanistically, CRTI is an oxidase that transfers the electrons from phytoene directly to oxygen, forming water [20]. In contrast, all evidence accumulated so far indicates the PDS-mediated plant-type desaturation to interact with oxygen only indirectly, through PTOX, using plastoquinone as an intermediate electron carrier [14,15]. Therefore, CRTI by itself is not a cause for any major Q/QH_2 imbalance. Since CRTI does not produce radicals [20], it is also not a source of the elevated ROS shown here. Therefore, reduced PDS involvement may either affect the redox state of quinones directly and much more profoundly than ever anticipated leading to redox-dependent retrograde signaling and the upregulation of PTOX levels and maybe, the transcriptional activation of other genes. Work has been initiated to clarify this issue.

However, there is a second property in which the two systems differ. CRTI catalyzes the introduction of all four double bonds needed to form all-*trans* lycopene in one step through all-*trans* configured (predominantly enzyme-bound) intermediates. In contrast, PDS requires a second desaturase, ζ-carotene desaturase (ZDS) and two *cis-trans* isomerases, namely ζ-carotene isomerase (ZISO) and carotene isomerase (CRTISO) to carry out a desaturation pathway that is characterized by poly-cis configured intermediates (see [53] for review), finally producing all-*trans* lycopene, like CRTI. In other words, expressing CRTI is expected to lower the rate of poly-*cis* carotene intermediate formation. The function of these plant-specific poly-*cis* carotene intermediates is not understood at present, however, evidence is accumulating that they are the source of regulatory molecules capable in modifying gene expression [54]. Work is in progress to identify this conceivable causal relationship.

In conclusion, our study on Arabidopsis plants that constitutively express CRTI provides evidence that the PTOX level is crucial for the balance between the different pathways of photosynthetic electron flow –linear, cyclic, Mehler reaction. The increase in the amount and activity of PTOX leads to a perturbation of the redox state of the photosynthetic electron transport chain and seems to be responsible for the increased susceptibility to light while the plants seem to cope well with the alteration in the carotenoid composition as seen by the small effects on maximum NPQ and the unchanged level of $^1O_2$ generation.

Acknowledgements

We thank B. Robert (CEA Saclay) for stimulating discussions and V. Mary (CEA Saclay) for excellent technical assistance. DG was supported by EU FP7 Marie Curie Initial Training Network HARVEST (FP7 project no. 238017). PB and PS were supported by the HarvestPlus consortium (www.harvestplus.org).

Appendix A. Supplementary data

Supplementary data to this article can be found online at http://dx.doi.org/10.1016/j.bbabio.2013.12.010.

References

[1] K. Sonoike, Photoinhibition of photosystem I, Physiol. Plant. 142 (2011) 56–64.
[2] I. Vass, Molecular mechanisms of photodamage in the photosystem II complex, Biochim. Biophys. Acta 1817 (2012) 209–217.
[3] A. Krieger-Lizskay, C. Fufezan, A. Trebst, Singlet oxygen production in photosystem II and related protection mechanism, Photosynth. Res. 98 (2008) 551–564.
[4] A. Krieger-Liszkay, P.B. Kós, E. Hideg, Superoxide anion radicals generated by methylviologen in photosystem I damage photosystem II, Physiol. Plant. 142 (2011) 17–25.

[5] N.R. Baker, J. Harbinson, D.M. Kramer, Determining the limitations and regulation of photosynthetic energy transduction in leaves, Plant Cell Environ. 30 (2007) 1107–1125.
[6] J.D. Rochaix, Regulation of photosynthetic electron transport, Biochim. Biophys. Acta 1807 (2011) 375–383.
[7] P. Müller, X.P. Li, K.K. Niyogi, Non-photochemical quenching, a response to excess light energy, Plant Physiol. 125 (2001) 1558–1566.
[8] B.J. Pogson, K.K. Niyogi, O. Björkman, D. DellaPenna, Altered xanthophyll compositions adversely affect chlorophyll accumulation and non-photochemical quenching in Arabidopsis mutants, Proc. Natl. Acad. Sci. U. S. A. 95 (1998) 13324–13329.
[9] B.J. Pogson, H.M. Rissler, Genetic manipulation of carotenoid biosynthesis and photoprotection, Philos. Trans. R. Soc. Lond. B Biol. Sci. 355 (2000) 1395–1403.
[10] C. Ilioaia, M.P. Johnson, P.N. Liao, A.A. Pascal, R. van Grondelle, P.J. Walla, A.V. Ruban, B. Robert, Photoprotection in plants involves a change in lutein 1 binding domain in the major light-harvesting complex of photosystem II, J. Biol. Chem. 286 (2011) 27247–27254.
[11] H. Lokstein, L. Tian, J.E. Polle, D. DellaPenna, Xanthophyll biosynthetic mutants of *Arabidopsis thaliana*: altered nonphotochemical quenching of chlorophyll fluorescence is due to changes in photosystem II antenna size and stability, Biochim. Biophys. Acta 1553 (2002) 309–319.
[12] P. Schaub, S. Al-Babili, R. Drake, P. Beyer, Why is golden rice golden (yellow) instead of red? Plant Physiol. 138 (2005) 441–450.
[13] G. Diretto, S. Al-Babili, R. Tavazza, V. Papacchioli, P. Beyer, G. Giuliano, Metabolic engineering of potato carotenoid content through tuber-specific overexpression of a bacterial mini-pathway, PLoS One 2 (2007).
[14] M.P. Mayer, P. Beyer, H. Kleinig, Quinone compounds are able to replace molecular oxygen as terminal electron acceptor in phytoene desaturation in chromoplasts of *Narcissus pseudonarcissus* L, Eur. J. Biochem. 191 (1990) 359–363.
[15] S.R. Norris, T.R. Barrette, D. DellaPenna, Genetic dissection of carotenoid synthesis in *Arabidopsis* defines plastoquinone as an essential component of phytoene desaturation, Plant Cell 7 (1995) 2139–2149.
[16] P. Carol, D. Stevenson, C. Bisanz, J. Breitenbach, G. Sandmann, R. Mache, C. Coupland, M. Kuntz, Mutations in the *Arabidopsis* gene IMMUTANS cause a variegated phenotype by inactivating a chloroplast terminal oxidase associated with phytoene desaturation, Plant Cell 11 (1999) 57–68.
[17] D. Wu, D.A. Wright, C. Wetzel, D.F. Voytas, S. Rodermel, The IMMUTANS variegation locus of *Arabidopsis* defines a mitochondrial alternative oxidase homolog that functions during early chloroplast biogenesis, Plant Cell 11 (1999) 43–55.
[18] E.M. Josse, A.J. Simkin, J. Gaffé, A.M. Labouré, M. Kuntz, P. Carol, A plastid terminal oxidase associated with carotenoid desaturation during chromoplast differentiation, Plant Physiol. 123 (2000) 1427–1436.
[19] S. Nashilevitz, C. Melamed-Bessudo, Y. Izkovich, I. Rogachev, S. Osorio, M. Itkin, A. Adato, I. Pankratov, J. Hirschberg, A.R. Fernie, S. Wolf, B. Usadel, A.A. Levy, D. Rumeau, A. Aharoni, An orange ripening mutant links plastid NAD(P)H dehydrogenase complex activity to central and specialized metabolism during tomato fruit maturation, Plant Cell 22 (2010) 1977–1997.
[20] P. Schaub, Q. Yu, S. Gemmecker, P. Poussin-Courmontagne, J. Mailliot, A.G. McEwen, S. Ghisla, S. Al-Babili, J. Cavarelli, P. Beyer, On the structure and function of the phytoene desaturase CRTI from *Pantoea ananatis*, a membrane-peripheral and FAD-dependent oxidase/isomerase, PLoS One 7 (2012).
[21] J.M. Ducruet, T. Miranda, Graphical and numerical analysis of thermoluminescence and fluorescence F_0 emission in photosynthetic material, Photosynth. Res. 33 (1992) 15–27.
[22] T. Roach, A. Krieger-Liszkay, The role of the PsbS protein in the protection of photosystems I and II against high light in *Arabidopsis thaliana*, Biochim. Biophys. Acta 1817 (2012) 2158–2165.
[23] E. Hideg, Z. Deák, M. Hakala-Yatkin, M. Karonen, A.W. Rutherford, E. Tyystjärvi, I. Vass, A. Krieger-Liszkay, Pure forms of the singlet oxygen sensors TEMP and TEMPD do not inhibit photosystem II, Biochim. Biophys. Acta 1807 (2011) 1658–1661.
[24] E.G. Andrizhiyevskaya, A. Chojnicka, J.A. Bautista, B.A. Diner, R. van Grondelle, J.P. Dekker, Origin of the F685 and F695 fluorescence in photosystem II, Photosynth. Res. 84 (2005) 173–180.
[25] K. Asada, K. Kiso, K. Yoshikawa, Univalent reduction of molecular oxygen by spinach chloroplasts on illumination, J. Biol. Chem. 249 (1974) 2175–2181.
[26] M.M. Mubarakshina, B.N. Ivanov, The production and scavenging of reactive oxygen species in the plastoquinone pool of chloroplast thylakoid membranes, Physiol. Plant. 140 (2010) 103–110.
[27] P. Pospíšil, Molecular mechanisms of production and scavenging of reactive oxygen species by photosystem II, Biochim. Biophys. Acta 1817 (2012) 218–231.
[28] E. Heyno, C.M. Gross, C. Laureau, M. Culcasi, S. Pietri, A. Krieger-Liszkay, Plastid alternative oxidase (PTOX) promotes oxidative stress when overexpressed in tobacco, J. Biol. Chem. 284 (2009) 31174–31180.
[29] N. Ahmad, F. Michoux, P.J. Nixon, Investigating the production of foreign membrane proteins in tobacco chloroplasts: expression of an algal plastid terminal oxidase, PLoS One 7 (2012).
[30] D. Rumeau, N. Bécuwe-Linka, A. Beyly, M. Louwagie, J. Garin, G. Peltier, New subunits NDH-M, -N, and -O, encoded by nuclear genes, are essential for plastid Ndh complex functioning in higher plants, Plant Cell 17 (2005) 219–232.
[31] A.W. Rutherford, A.R. Crofts, Y. Inoue, Thermoluminescence as a probe of photosystem II photochemistry—the origin of the flash-induced glow peaks, Biochim. Biophys. Acta 682 (1982) 457–465.
[32] J.M. Ducruet, Pitfalls, artefacts and open questions in chlorophyll thermoluminescence of leaves or algal cells, Photosynth. Res. 115 (2013) 89–99.
[33] V.N. Peeva, S.Z. Tóth, G. Cornic, J.M. Ducruet, Thermoluminescence and P700 redox kinetics as complementary tools to investigate the cyclic/chlororespiratory electron pathways in stress conditions in barley leaves, Physiol. Plant. 144 (2012) 83–97.
[34] A. Krieger, S. Bolte, K.J. Dietz, J.M. Ducruet, Thermoluminescence studies on the facultative CAM plant *Mesembryanthemum crystallinum*, Planta 205 (1998) 587–594.
[35] A.P. Hertle, T. Blunder, T. Wunder, P. Pesaresi, M. Pribil, U. Armbruster, D. Leister, PGRL1 is the elusive ferredoxin-plastoquinone reductase in photosynthetic cyclic electron flow, Mol. Cell 49 (2013) 511–523.
[36] G.N. Johnson, Reprint of: physiology of PSI cyclic electron transport in higher plants, Biochim. Biophys. Acta 1807 (2011) 906–911.
[37] D. Rumeau, G. Peltier, L. Cournac, Chlororespiration and cyclic electron flow around PSI during photosynthesis and plant stress response, Plant Cell Environ. 30 (2007) 1041–1051.
[38] P. Streb, E.-M. Josse, E. Gallouët, F. Baptist, M. Kuntz, G. Cornic, Evidence for alternative electron sinks to photosynthetic carbon assimilation in the high mountain plant species *Ranunculus glacialis*, Plant Cell Environ. 28 (2005) 1123–1135.
[39] C. Laureau, R. De Paepe, G. Latouche, M. Moreno-Chacón, G. Finazzi, M. Kuntz, G. Cornic, P. Streb, Plastid terminal oxidase (PTOX) has the potential to act as a safety valve for excess excitation energy in the alpine plant species *Ranunculus glacialis* L, Plant Cell Environ. (2013), http://dx.doi.org/10.1111/pce.12059(in press).
[40] M.J. Quiles, Stimulation of chlororespiration by heat and high light intensity in oat plants, Plant Cell Environ. 29 (2006) 1463–1470.
[41] L.V. Savitch, A.G. Ivanov, M. Krol, D.P. Sprott, G. Öquist, N.P.A. Huner, Regulation of energy partitioning and alternative electron transport pathways during cold acclimation of lodgepole pine is oxygen dependent, Plant Cell Physiol. 51 (2010) 1555–1570.
[42] P. Stepien, G.N. Johnson, Contrasting responses of photosynthesis to salt stress in the glycophyte Arabidopsis and the halophyte Thellungiella: role of the plastid terminal oxidase as an alternative electron sink, Plant Physiol. 149 (2009) 1154–1165.
[43] D. Rosso, A.G. Ivanov, A. Fu, J. Geisler-Lee, L. Hendrickson, M. Geisler, G. Stewart, M. Krol, V. Hurry, S.R. Rodermel, D.P. Maxwell, N.P. Hüner, IMMUTANS does not act as a stress-induced safety valve in the protection of the photosynthetic apparatus of Arabidopsis during steady-state photosynthesis, Plant Physiol. 142 (2006) 574–585.
[44] Y. Munekage, M. Hojo, J. Meurer, T. Endo, M. Tasaka, T. Shikanai, PGR5 is involved in cyclic electron flow around photosystem I and is essential for photoprotection in Arabidopsis, Cell 110 (2002) 361–371.
[45] Y.N. Munekage, B. Genty, G. Peltier, Effect of PGR5 impairment on photosynthesis and growth in *Arabidopsis thaliana*, Plant Cell Physiol. 49 (2008) 1688–1698.
[46] P. Joliot, G.N. Johnson, Regulation of cyclic and linear electron flow in higher plants, Proc. Natl. Acad. Sci. U. S. A. 108 (2011) 13317–13322.
[47] C.M. Wetzel, C.Z. Jiang, L.J. Meehan, D.F. Voytas, S.R. Rodermel, Nuclear-organelle interactions: the immutans variegation mutant of Arabidopsis is plastid autonomous and impaired in carotenoid biosynthesis, Plant J. 6 (1994) 161–175.
[48] A. Foudree, A. Putarjunan, S. Kambakam, T. Nolan, J. Fussell, G. Pogorelko, S. Rodermel, The mechanism of variegation in Immutans provides insights into chloroplast biogenesis, Front. Plant. Sci. 3 (2012) 260.
[49] Y. Okegawa, Y. Kobayashi, T. Shikanai, Physiological links among alternative electron transport pathways that reduce and oxidize plastoquinone in Arabidopsis, Plant J. 63 (2010) 458–468.
[50] M. Trouillard, M. Shahbazi, L. Moyet, F. Rappaport, P. Joliot, M. Kuntz, G. Finazzi, Kinetic properties and physiological role of the plastoquinone terminal oxidase (PTOX) in a vascular plant, Biochim. Biophys. Acta 1817 (2012) 2140–2148.
[51] A.M. Lennon, P. Prommeenate, P.J. Nixon, Location, expression and orientation of the putative chlororespiratory enzymes, Ndh and IMMUTANS, in higher-plant plastids, Planta 218 (2003) 254–260.
[52] M. Iwai, K. Takizawa, R. Tokutsu, A. Okamuro, Y. Takahashi, J. Minagawa, Isolation of the elusive supercomplex that drives cyclic electron flow in photosynthesis, Nature 464 (2010) 1210–1213.
[53] C.I. Cazzonelli, Carotenoids in nature: insights from plants and beyond, Funct. Plant Biol. 38 (2011) 833–847.
[54] D.E. Kachanovsky, S. Filler, T. Isaacson, J. Hirschberg, Epistasis in tomato color mutations involves regulation of phytoene synthase 1 expression by cis-carotenoids, Proc. Natl. Acad. Sci. U. S. A. 109 (2012) 19021–19026.